12th IFAC International Symposium on
Advanced Control of Chemical Processes
July 14-17, 2024. Toronto, Canada

Model reduction for soil moisture and hydraulic parameter estimation using sequential triggers

Sarupa Debnath * **Soumya R. Sahoo** * **Bernard T. Agyeman** *
Xunyuan Yin ** **Jinfeng Liu** *

* *Department of Chemical and Materials Engineering, University of Alberta, Edmonton, Canada T6G 1H9 (Email: jinfeng@ualberta.ca)*
** *School of Chemistry, Chemical Engineering & Biotechnology, Nanyang Technological University, 62 Nanyang Drive, Singapore, 637459, Singapore*

Abstract: In this study, we introduce a triggered model reduction method for soil moisture and hydraulic parameter estimation. The approach employs cluster-based unsupervised learning to extract simplified models capturing essential dynamics of the complex original nonlinear system. To handle model mismatch over time, a sequential triggering method with an event trigger followed by a performance trigger is proposed for model identification. Further, an adaptive extended Kalman filter (EKF) that can take advantage of the adaptively reduced models is developed to estimate soil moisture and the associated hydraulic parameters. The performance of the proposed method is illustrated based on a large-scale agricultural field.

Keywords: Hierarchical clustering; sequential triggering; adaptive reduced-order estimator; large scale system; nonlinear systems.

1. INTRODUCTION

Many dynamical systems are of high dimensions, with governing equations complex and nonlinear. Agro-hydrological systems are examples of such systems. The complexity of these models poses challenges in performing simulations, model-based optimization, control and estimation. This motivates researchers to develop model reduction methods to reduce the model complexity.

Over the last few decades, different dimensionality reduction methods have been discussed in control theory and applied to control systems for many engineering applications. Popular techniques for model reduction in dynamical systems include subsystem decomposition (Debnath et al., 2022), proper orthogonal decomposition (POD), and Krylov methods (Antoulas, 2005). These methods are used to develop models of lower dimensions compared with the original models and the reduced model can then be used in the design of controllers and estimators. In Sahoo et al. (2022a), a cluster-based model reduction approach is proposed that preserves the overall connection among states of the original systems. This technique gives non-overlapping clusters, where states within each cluster follow similar trajectories and thus are represented by a reduced-order state. This guarantees the retention of dynamic properties and physical topology within the reduced-order model.

An agro-hydrological system describes water movements in the soil and plant. The modeling of the water dynamics in an agro-hydrological system typically involves the Richards equation, which is a partial differential equation. For large-scale agricultural fields, this leads to high-dimensional problems, which pose significant challenges when such a model is used in the design of estimation and control algorithms (Sahoo et al., 2022b). In this work, we propose an adaptive model reduction approach to address the high dimensionality issue associated with agro-hydrological models based on the Richards equation.

In our previous work (Debnath et al., 2023), a performance-triggered model reduction method for soil moisture estimation was proposed. The method in Debnath et al. (2023) uses a cluster-based model reduction approach and is specifically developed for point sensors that provide continuously available measurements. This work extends the method to present a sequentially triggered model reduction approach for simultaneous soil moisture and hydraulic parameter estimation. In this work, instead of point sensors, we consider intermittent measurements obtained from microwave radiometers mounted on a rotating center pivot irrigation system. The intermittent nature of the microwave measurements introduces further challenges in the design of the triggering mechanism, which makes the performance-based triggering mechanism developed in (Debnath et al., 2023) not implementable. The work proposes a sequence of triggers for model reduction. The proposed method is also illustrated based on measurements obtained from an actual agricultural field.

⋆ Financial support from Natural Sciences and Engineering Research Council of Canada, Alberta Innovates, and Academic Research Fund Tier 1 (RG63/22) of the Ministry of Education, Singapore is gratefully acknowledged.

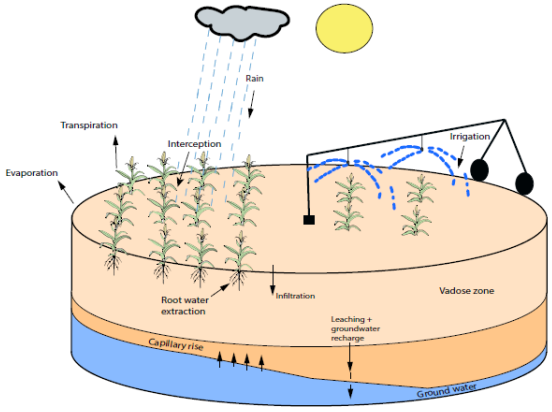

Fig. 1. Considered agro-hydrological system (Agyeman et al., 2021).

2. PRELIMINARIES

2.1 Agro-hydrological systems description

The agro-hydrological system considered in this work is equipped with a center pivot irrigation system as shown in Fig. 1. The hydrological cycle in the system involves soil, crops, the atmosphere, and water. The dynamics of water infiltration into the soil, driven by capillary and gravitational forces, is characterized by the Richards equation (Richards, 1931). A cylindrical version of the Richards equation is used to facilitate the consideration of the movement of the center pivot irrigation system. The cylindrical version of the Richards equation is shown as follows (Agyeman et al., 2021):

$$\frac{\partial \theta_m}{\partial t} = c(h)\frac{\partial h}{\partial t} = \frac{1}{r}\frac{\partial}{\partial r}\left[rK(h)\frac{\partial h}{\partial r}\right] + \frac{1}{r}\frac{\partial}{\partial \theta}\left[\frac{K(h)}{r}\frac{\partial h}{\partial \theta}\right] + \frac{\partial}{\partial z}\left[K(h)\left(\frac{\partial h}{\partial z}+1\right)\right] - S(h,z) \quad (1)$$

where θ_m [$\mathrm{m^3m^{-3}}$] and h [m] represent the field water soil moisture content and pressure head, $c(h)$ [$\mathrm{m^{-1}}$] and $K(h)$ [$\mathrm{ms^{-1}}$] denote the soil water capacity and hydraulic conductivity, while r [m], θ [rad], and z [m] are the radial, azimuthal, and axial spatial variables, respectively, and $S(h,z)$ [$\mathrm{m^3m^{-3}s^{-1}}$] is the sink term. The conversion from h to θ_m can be referenced in Agyeman et al. (2021).

2.2 State space model

We consider an explicit finite difference method for spatially discretizing system (1), resulting in a continuous-time state-space representation as follows:

$$\dot{x}(t) = f(x(t), p(t), u(t)) + w(t) \quad (2a)$$
$$y(t) = Cx(t) + v(t) \quad (2b)$$

where $x(t) \in \mathbb{R}^{N_x}$ represents state vector of the pressure head, $p(t) \in \mathbb{R}^{N_p}$ is the soil hydraulic parameter vector, and $u \in \mathbb{R}^{N_u}$ denotes the total precipitation includes applied irrigation and rain, $y(t) \in \mathbb{R}^{N_y}$ is the vector of measurements of soil moisture content, $w(t) \in \mathbb{R}^{N_x}$ denotes the system disturbance, where C is a matrix relates x and y, and $v(t) \in \mathbb{R}^{N_y}$ is the measurement noise.

Figure 2 shows an illustration of the discretization of system (1), which is discretized into a total of N_x nodes

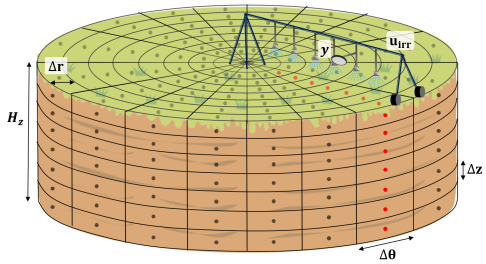

Fig. 2. Discretization of the agro-hydrological system.

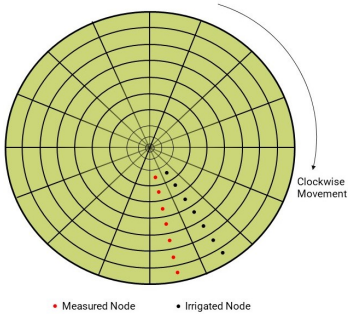

Fig. 3. Center pivot with microwave sensors (top-view).

with N_r, N_θ, and N_z in the radial, azimuthal, and axial directions, respectively. The dimension of the irrigation u_{irr} is the same as the radial N_r nodes. The soil moisture observation is obtained from the microwave radiometers which are installed on the center pivot system and the measurements are obtained intermittently. As the center pivot irrigates the field, the microwave radiometer rotates and provides the soil moisture observations shown in Fig. 3. The matrix C is sparse because the number of measurements is much less than the number of nodes $N_y << N_x$. Also, it is changing due to the rotation of the center pivot which results in changing in the measurement locations. Owing to the heterogeneity of soil texture, each discrete node is assigned its unique set of parameters. In this work, we examined five crucial soil hydraulic parameters: K_s, θ_s, θ_r, α, and η, for each discretized node (Agyeman et al., 2023). We also assume that soil properties vary similarly at different depths within the soil.

2.3 Objective

The main objective is to estimate the soil moisture content θ_m at each node across the field using soil moisture measurements from microwave radiometers. A center pivot irrigation system rotates across the field slowly. It typically takes more than one day for a center pivot to complete one cycle. The estimation of the soil moisture and hydraulic parameters using these microwave measurements poses a few challenges including (a) the computational complexity of the Richards model in estimation methods, and (b) the low degree of observability of x with limited observations.

3. PROPOSED APPROACH

To handle the challenges, we propose an information fusion system, data assimilation (Agyeman et al., 2023), within an adaptive reduced model framework as illustrated in Fig. 4. The availability of measurements, acting as an event trigger, guides the decision-making process, determining

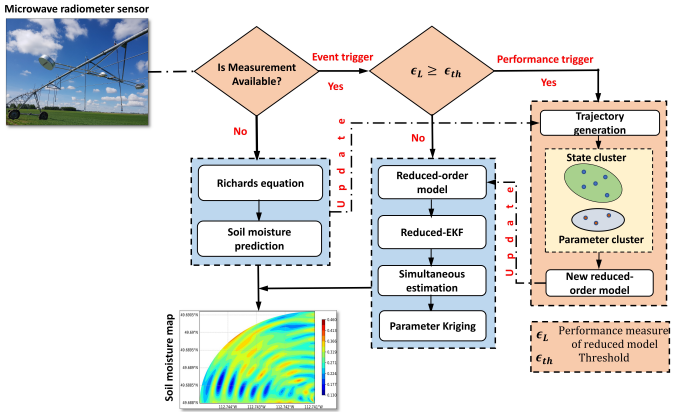

Fig. 4. The proposed adaptive model reduction and data assimilation.

whether to pursue open-loop predictions employing the Richards equation or opt for simultaneous estimation using a reduced-order model. Sequentially, the prediction performance of the existing reduced model is assessed, and only the reduced-order model exhibiting inadequate performance is replaced with a new model in real time. The state trajectory is generated based on the current estimates or predicted soil moisture information. Subsequently, clusters are formed using the hierarchical clustering method, separately identifying clusters for both states and parameters. These trajectories are developed with consideration of anticipated irrigation, rainfall, evapotranspiration (ET), and crop coefficient (K_c) over three days. Utilizing the reduced-order model, we construct a reduced-order estimator through an EKF algorithm for simultaneous estimation of soil water and its parameters. Parameters chosen for estimation are those associated with nodes where measurements are available during the sampling period, as discussed in Orouskhani et al. (2022). The estimable parameters denoted by $p^e \in \mathbb{R}^{N_{pe}}$ and the rest of the parameters are kept in $p^{ne} \in \mathbb{R}^{N_{pn}}$ ($p = [p^{e,T} \;\; p^{ne,T}]^T$). To update the non-estimable parameters, estimated parameters are interpolated using the Kriging method.

3.1 Proposed adaptive model reduction

To identify the reduced model at the beginning or to re-identify a model when $\epsilon_L \geq \epsilon_{th}$ as illustrated in Fig. 2, the same steps are followed and explained below:

State trajectory generation: The current state estimates at t_k, $\hat{x}(t_k)$, is assumed as the initial soil moisture condition, and the system (2) is simulated with forecast data and prescribed irrigation for the following N_{fd} steps.

$$X_m = [x(t_k) \; x(t_{k+1}) \; \ldots \; x(t_{k+N_{fd}})]$$

where $X_m \in \mathbb{R}^{N_x \times N_{fd}}$ is the snapshot matrix of the soil water for the m^{th} model reduction considering that $(m-1)$ number of model reductions were performed before t_k.

$$P_m = [K_s(t_k), \theta_s(t_k), \theta_r(t_k), \alpha(t_k), \eta(t_k)]$$

where P_m is the current parameter estimate at t_k.

Generation of state and parameter clusters: Agglomerate hierarchical clustering is used to group state trajectories into clusters based on their similarity. Each row in X_m implies a state trajectory and is considered a data point. For example, the trajectory of a state, $\bar{x}_i$ is denoted as data point i ($i = 1, \ldots, N_x$). Each data point (state trajectory) is considered a cluster, and the distances between these clusters are calculated. When the average distance between data points is smaller than a threshold th_x, a cluster tuning parameter, they remain in one cluster (Steinbach et al., 2000). Let's consider two clusters p and q with sizes n_p, and n_q respectively. The measure of the distance between clusters p and q is evaluated using Euclidean distance denoted by d as follows:

$$\mathscr{D}(p,q) = \frac{1}{n_p n_q} \sum_{i=1}^{n_p} \sum_{j=1}^{n_q} d(\bar{x}_{pi}, \bar{x}_{qj})$$

where $\bar{x}_{pi}$ and $\bar{x}_{qj}$ denote data points within clusters p and q respectively. Similarly, each parameter in P_m is clustered with a distance threshold th_p which is also a cluster tuning parameter.

Consider that there are r_m clusters during the m^{th} model reduction. The collection of clusters for the m^{th} model is denoted as: $C^{(m)} = \{C_1^{(m)}, C_2^{(m)}, \ldots, C_{r_m}^{(m)}\}$ as . The clusters must satisfy two properties: a) $C_i^{(m)} \cap C_j^{(m)} = \Phi$ and b) $C_1^{(m)} \cup C_2^{(m)} \cup \ldots \cup C_{r_m}^{(m)} = X_m$. In this study, we used Petrov-Galerkin projection for the reduced model (Antoulas, 2005). The projection matrix ($U_x^{(m)} \in \mathbb{R}^{N_x \times r_m}$) is constructed using the formed clusters ($C^{(m)}$) and the entries of the matrix are evaluated below:

$$U_{x(i,j)}^{(m)} = \begin{cases} v_i, & \text{when point } i \in C_j^{(m)} \\ 0, & \text{otherwise} \end{cases}$$

and v_i is defined as follows:

$$v_i = 1/||\beta_i||, \;\; \beta_i = \mathbb{S}_i^T \beta$$

where $||\beta_i||$ is the norm L_2 of β_i which is defined by $\beta = [1, \ldots, 1]^T \in \mathbb{R}^{N_x}$. $\mathbb{S}_i = s_{C_i} \in \mathbb{R}^{N_x \times N_{C_i}}$, where N_{C_i} is the of number of nodes belongs to cluster C_i. $\mathbb{S}$ is a matrix with columns made of s_j's and every s_j is the j-th column of the identity matrix $\mathbb{I}_{N_x \times N_x}$. Likewise, when there are p_m clusters for parameters during the m^{th} model reduction, the projection matrix $U_p \in \mathbb{R}^{N_p \times p_m}$ is constructed for the parameter clusters.

Augmented reduced state and parameter model: The augmented model is obtained by combining equation (2) and $\dot{p}(t) = 0$ as follows:

$$\dot{x}_a(t) = f_a(x_a(t), u(t)) + w_a(t) \tag{3a}$$
$$y(t) = C_a x_a(t) + v_a(t) \tag{3b}$$

where subscript a indicates the augmentation and $x_a(t) = [x(t)^T \;\; p(t)^T]^T$. The total augmentation is necessary for updating the covariance matrix in EKF, simplifying the calculation of the simultaneous estimation. However, the non-estimable parameters p^{ne} are assigned nominal values while estimating x_a. For the augmented reduced model we define the augmented projection $U \in \mathbb{R}^{(N_x+N_p)\times(r_m+p_m)}$ after m^{th} model reduction as a block diagonal matrix $U^m = blkdiag\{[U_x^m], [U_p^m]\}$.

Reduced state space model: We consider a discrete-time reduced state space model for the augmented model (3) as follows:

$$\xi^{(m)}(t_{k+1}) = f_{rd}^{(m)}(\xi^{(m)}(t_k), u(t_k), w_a(t_k)) \tag{4a}$$
$$y(t_k) = C_r^{(m)} \xi^{(m)}(t_k) + v_a(t_k) \tag{4b}$$

where ξ is the reduced state, f_{rd} is the discrete-time function of the reduced model and $C_r^{(m)} = C_a U^{(m)T}$.

The projection is performed as $\xi^{(m)}(t) = U^{(m)T}x_a(t)$, and $f_r^{(m)} = U^{(m)T}f_a$ and the approximated predicted state is evaluated as $\tilde{x}_a(t) = U^{(m)}\xi^{(m)}$. To maintain a consistent flow of information between the reduced models, the $(m-1)^{th}$ model is reverted to the full-order system and subsequently projected to the m^{th} model using the updated projection matrix.

Proposed extended Kalman filter: The EKF begins with an initial guess for the state $\hat{x}_a(t_0)$ and its covariance matrix $P_a(t_0)$ by employing $\hat{\xi}^{(m)}(t_0) = U^{(m)T}\hat{x}_a(t_0)$ and $P_r(t_0) = U^{(m)}P_a(t_0)U^{(m)T}$. In the prediction step, the reduced state $\xi^{(m)}$ and reduced covariance matrix $P_r^{(m)}$ are predicted based on the reduced model (4) at t_k below:

$$\hat{\xi}^{(m)}(t_{k|k-1}) = f_{rd}^{(m)}(\hat{\xi}^{(m)}(t_{k-1}), u(t_{k-1}), w_a(t_{k-1}))$$
$$P_r^{(m)}(t_{k|k-1}) = A_d^{(m)}(t_{k-1})P_r^{(m)}(t_{k-1})A_d^{(m)}(t_{k-1}) + Q_r^{(m)}$$

where $\hat{\xi}^{(m)}(t_{k|k-1})$ denotes the reduced state prediction at t_k based on the previous reduced estimate at t_{k-1}, and $A_d^{(m)}(t_{k-1}) = \left.\frac{\partial f_{rd}^{(m)}}{\partial \xi^{(m)}}\right|_{\hat{\xi}^{(m)}(t_{k-1})}$ is the state-transition matrix obtained by linearizing the nonlinear reduced model (4). $Q_r^{(m)}$ is the reduced covariance matrix for the process disturbance where $Q_r^{(m)} = U^{(m)}Q_aU^{(m)T}$, and Q_a is the augmented system covariance matrix of w_a. In the update step, the predicted reduced state and its reduced covariance matrix are updated based on the measurements.

$$\hat{\xi}^{(m)}(t_k) = \hat{\xi}^{(m)}(t_{k|k-1}) + K_r^{(m)}(t_k)(y(t_k) - C_r^{(m)}\hat{\xi}^{(m)}(t_{k|k-1}))$$
$$P_r^{(m)}(t_k) = (I_{r_m} - K_r^{(m)}(t_k)C_r^{(m)})P_r^{(m)}(t_{k|k-1})$$

where $\hat{\xi}^{(m)}(t_k)$ and $P_r^{(m)}(t_k)$ represent the estimated reduced state and the *posteriori* reduced covariance matrix at t_k respectively. $K_r^{(m)}(t_k)$ denotes the Kalman gain utilized to minimize the *a posteriori* error covariance based on the measurement innovation $y(t_k) - C_r^{(m)}\hat{\xi}^{(m)}(t_{k|k-1})$ and I_{r_m} represents the identity matrix of the m^{th} reduced model of dimesion r_m. The Kalman gain is evaluated as follows:

$$K_r^{(m)}(t_k) = P_r^{(m)}(t_{k|k-1})C_r^{(m)T}(R + C_r^{(m)}P_r^{(m)}(t_{k|k-1})C_r^{(m)T})^{-1}$$

where R represents the covariance matrix of the measurement noise. Notably, $P_a(t_0)$, Q_a, and R serve as three tuning parameters for the EKF. The soil moisture and its parameter estimates from the reduced estimator are evaluated as $\hat{x}_r(t_k) = U^{(m)}\hat{\xi}^{(m)}(t_k)$. During model change, the information of the EKF is transferred as follows:

- Converting the reduced state and state covariance to the full order state and covariance: $\hat{x}_r = U^{(m-1)}\hat{\xi}^{(m-1)}$, $P_a = U^{(m-1)T}P_r^{(m-1)}U^{(m-1)}$.
- Projecting the full order information to the new reduced model: $\hat{\xi}^{(m)} = U^{(m)T}\hat{x}_r$, $P_r^{(m)} = U^{(m)}PU^{(m)T}$.

Design of the triggered metrics: The event trigger is a binary decision: when measurements are available, the EKF will be executed; otherwise, the open-loop prediction will be computed. We calculate the performance metric ϵ_L at t_k inspired by Alanqar et al. (2017) as follows:

Fig. 5. Investigated area in Lethbridge, Alberta, Canada.

$$\epsilon_L(t_k) = \frac{1}{N_d}\frac{100}{N_x + N_p}\sum_{j=1}^{N_d}\sum_{i=1}^{N_x+N_p}|\tilde{x}_{ai}(t_{k+j}) - x_{ai}(t_{k+j})|$$

where $\tilde{x}_{ai}$ and x_{ai} denote the open loop predictions of i^{th} node from the reduced model and the Richards equation respectively. A prediction horizon N_d is used for a day.

4. REAL CASE STUDY

The Research Farm operated by Lethbridge College is located in Lethbridge, Canada, and a quadrant of the field is chosen as shown in Fig. 5. The field primarily consists of clayey loam soil, with a few scattered sand lenses. The field is a circular field equipped with a five-span center pivot system. The microwave radiometers are installed on the center pivot system to observe soil moisture at various points during the rotation cycle and the soil moisture observations used in the study are collected in the summer of 2022. The soil parameter K_s is shown in Fig. 6(a) which varies across the field. The quadrant being studied has a radius of approximately 290 meters and a depth of 0.32 meters. The boundary conditions used in Richards equation for a quadrant can be found in Agyeman et al. (2021). We discretize the radius, angle, and depth into 30, 17, and 10 equally spaced sectors, respectively. Hence, the quadrant is discretized into total $N_x = 5100$ states and the total number of parameters is $N_p = 2550$ giving in total of 7650 estimates. The model undergoes temporal discretization with a step size of 30 minutes. In solving the Richards equation, we employ a symbolic CasADi integrator, specifically an explicit Runge-Kutta (RK4) method (Andersson et al., 2019). This symbolic approach with CasADi simplifies the computation of the necessary Jacobian matrices for implementing the EKF.

The soil moisture content measurements are considered from July 1^{st}, 2022 to August 8^{th}, 2022 in the investigated quadrant in this study. The soil moisture measurements are obtained from the microwave radiometers every 30 minutes. Data assimilation is carried out using $\frac{4}{5}^{th}$ of the measurement for training and the rest is used for validation. The raw measurements undergo multiple data pre-processing steps such as sorting the measurements by date and time, grouping them by quadrants, removing outliers, and mapping the measurements to the nodes of the model are explained explicitly in our previous work (Agyeman et al., 2023). Daily reference evapotranspiration (ET), rain, irrigation application, and crop coefficient (K_c) values which are crucial inputs into the field model, are

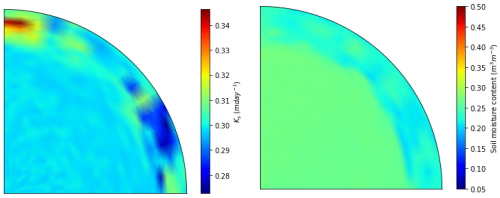

(a) (b)

Fig. 6. Spatial distribution of (a) the nominal (K_s) and (b) initial guess $\hat{\theta}_m$.

acquired from the Alberta Information Service website and Alberta Irrigation Center (Agyeman et al., 2023).

The proposed adaptive model reduction strategy utilizes distinct thresholds for cluster generation. We set th_x to 0.01 for the state and th_p to 0.0005 for the parameters. As the model changes, a trajectory spanning three days ($N_{fd} = 144$) is generated to account for the extended prediction horizon. The criteria for performance assessment consider the prediction for the following day ($N_d = 48$). To set the performance threshold, we find an appropriate threshold for the reduced model's performance at $\epsilon_{th} = 3$.

The reduced estimator is initialized with initial guess $\hat{x}_a(t_0)$ which is set with limited knowledge about the actual condition $x_a(t_0)$ shown in Fig. 6(b). In our prior study (Agyeman et al., 2023), we determined the parameter values for quadrant 4. In this current work, we make an informed initial guess for the parameters by leveraging the similarities in soil type. The initial covariance matrix $P_a(t_0)$ is a matrix with higher diagonal elements than the off-diagonal elements to account for the high uncertainty in $\hat{x}_a(t_0)$. In particular, the elements corresponding to the states are initialized in a range of $0.1 - 1700$, while those corresponding to the parameters are set to 5. The covariance matrices of process disturbance $Q = 0.008 I_{N_x+N_p}$ and measurement noise $R = 0.01 I_{N_y}$ are considered tuning parameters where I is the identity matrix.

The proposed approach is compared to a full estimator utilizing full model (3) and their performance is quantified using the Normalized Root Mean Square Error (NRMSE) as follows:

$$NRMSE = \frac{1}{(y_{max} - y_{min})} \sqrt{\frac{\sum_{k=1}^{N_y^v} (y(t_k) - \hat{y}(t_k))}{N_y^v}}$$

where $\hat{y}(t_k)$ and $y(t_k)$ are the estimated soil moisture content and measured soil moisture content, N_y^v represents the number of measurements within the validation dataset, and y_{max} and y_{min} are the highest and lowest soil moisture content in the validation set, respectively.

Figure 7 provides a comprehensive summary of the results found through the proposed model reduction approach. The occurrence of an event trigger, followed by a performance trigger, signals the necessity for a model adjustment. Out of fifteen available days with soil measurements, performance triggers are activated seven times in plot (a). It is evident that the threshold is violated six times, resulting in the re-identification of a reduced model on each occasion. The tuning parameters for the

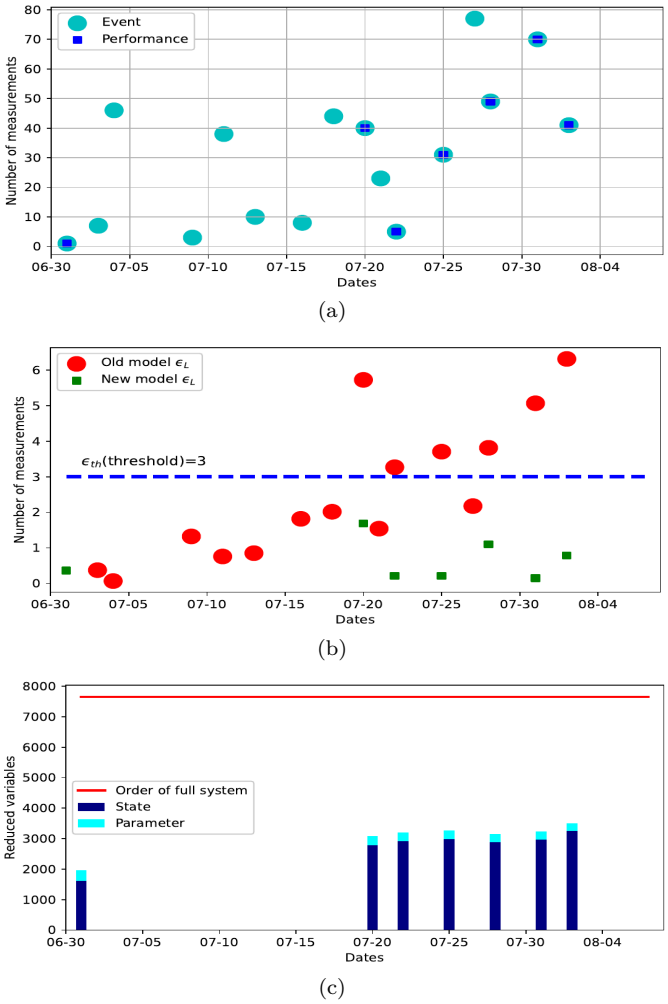

Fig. 7. (a) Triggers with measurements for training of EKF, (b) Performance measure, and (c) Reduced state and parameter order of adaptive models.

Table 1. Computational speed per iteration

[in Sec]	Data assimilation	Estimation
Reduced estimation	3.5 ± 0.4	$30 - 100$
Full estimation	7.4 ± 0.6	220 ± 40

cluster generation are set to ensure that the new model's metrics fall within the specified threshold in plot (b). The maximum model order is recorded as 3507 (3260, and 247), while the minimum model order stands at 1969 (1619, and 350) in plot (c). In Table 1, the simulation time required for estimation at each sampling point varies from 30 s for model orders around 2000 to 100 s for model orders around 3500. However, the full-order system with 7650 variables takes more than twice as long compared to the highest-ordered reduced model. Additionally, as the system variables increase, the simulation time for the large state-transition matrix, A_d, grows substantially. For the same reason, employing the EKF in the large-scale field becomes nearly intractable with the available computational resources. On average, the reduced estimator can provide assimilated soil moisture in just 3.5 s, while the full estimation takes approximately 7.4 s, and a computational efficiency of over 50% is achieved. This is why the reduced

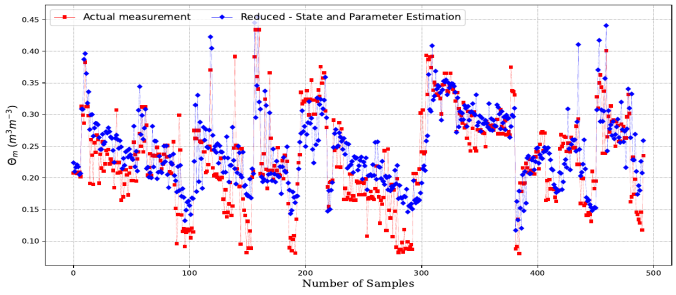

(a)

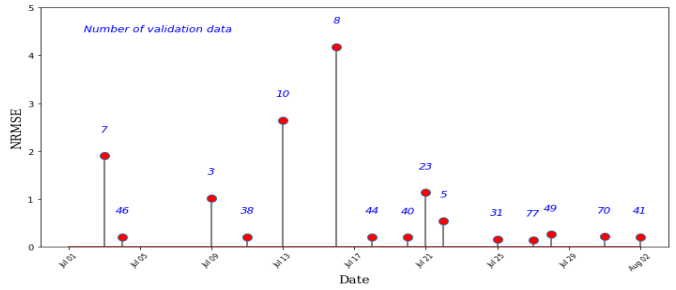

(b)

Fig. 8. (a) Actual measurements vs reduced estimation for the entire season with overall NRMSE= 0.1385, and (b) Day-wise NRMSE.

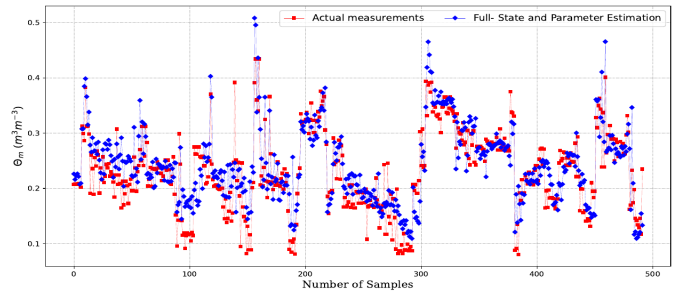

(a)

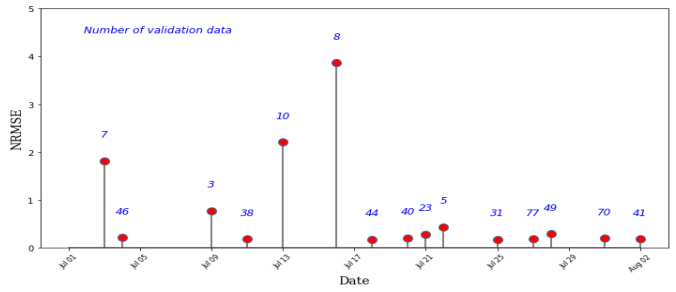

(b)

Fig. 9. (a) Actual measurements vs full estimation for the entire season with overall NRMSE= 0.1244, and (b) Day-wise NRMSE.

approach highly feasible approach for application in the large-scale field.

In Fig. 8(a) and Fig. 9(a), we achieve overall NRMSE values of 0.1385 and 0.1244 for the reduced and full-order estimations, respectively. However, it highlights a discrepancy of approximately 12 % in the cross-validation results, which corresponds to model approximation errors. When examining the daily NRMSE in Fig. 8(b) and Fig. 9(b), we realize that a limited number of measurements can result in decreased accuracy. Also, a similar error pattern is observed on most days, except for the 21^{st} and the following day, which could be due to a potential model-plant mismatch.

5. CONCLUSIONS

We address the challenge of high dimensionality of agro-hydrological model in its application to soil moisture and hydraulic parameter estimation. We leverage a sequential trigger approach to systematically deduce the reduced model. The reduced state estimator demonstrates satisfactory performance, providing both reasonable accuracy and improved computational speed.

REFERENCES

Agyeman, B.T., Bo, S., Sahoo, S.R., Yin, X., Liu, J., and Shah, S.L. (2021). Soil moisture map construction by sequential data assimilation using an extended kalman filter. *Journal of Hydrology*, 598, 126425.

Agyeman, B.T., Orouskhani, E., Naouri, M., Appels, W., Wolleben, M., Liu, J., and Shah, S.L. (2023). Maximizing soil moisture estimation accuracy through simultaneous hydraulic parameter estimation using microwave remote sensing: Methodology and application. *arXiv preprint arXiv:2305.15549*.

Alanqar, A., Durand, H., and Christofides, P.D. (2017). Error-triggered online model identification for model-based feedback control. *AIChE Journal*, 63(3), 949–966.

Andersson, J.A., Gillis, J., Horn, G., Rawlings, J.B., and Diehl, M. (2019). Casadi: a software framework for nonlinear optimization and optimal control. *Mathematical Programming Computation*, 11, 1–36.

Antoulas, A.C. (2005). *Approximation of large-scale dynamical systems*. SIAM.

Debnath, S., Sahoo, S.R., Agyeman, B.T., Yin, X., and Liu, J. (2023). An error-triggered adaptive model reduction and soil moisture estimation for agro-hydrological system. In *2023 62nd IEEE Conference on Decision and Control (CDC)*, 7586–7591. IEEE.

Debnath, S., Sahoo, S.R., Decardi-Nelson, B., and Liu, J. (2022). Subsystem decomposition and distributed state estimation of nonlinear processes with implicit time-scale multiplicity. *AIChE Journal*, 68(5), e17661.

Orouskhani, E., Agyeman, B.T., and Liu, J. (2022). Simultaneous estimation of soil moisture and hydraulic parameters for precision agriculture. part a: Methodology. In *2022 IEEE International Symposium on Advanced Control of Industrial Processes (AdCONIP)*, 12–17. IEEE.

Richards, L.A. (1931). Capillary conduction of liquids through porous mediums. *Physics*, 1(5), 318–333.

Sahoo, S.R., Agyeman, B.T., Debnath, S., and Liu, J. (2022a). Knowledge-based optimal irrigation scheduling of agro-hydrological systems. *Sustainability*, 14(3), 1304.

Sahoo, S.R., Agyeman, B.T., Debnath, S., and Liu, J. (2022b). Knowledge-based optimal irrigation scheduling of three-dimensional agro-hydrological systems. *IFAC-PapersOnLine*, 55(7), 441–446.

Steinbach, M., Karypis, G., and Kumar, V. (2000). A comparison of document clustering techniques. *CS&E Technical Reports*.